Available online at www.sciencedirect.com
SCIENCE DIRECT®
Nuclear Instruments and Methods in Physics Research B 249 (2006) 6–12
NIM B
Beam Interactions with Materials & Atoms
www.elsevier.com/locate/nimb

Allotropic effects on the energy loss of swift H^+ and He^+ ion beams through thin foils

Rafael Garcia-Molina [a,*], Isabel Abril [b], Cristian D. Denton [b], Santiago Heredia-Avalos [a]

[a] Departamento de Física, Universidad de Murcia, Apartado 4021, E-30080 Murcia, Spain
[b] Departament de Física Aplicada, Universitat d'Alacant, Apartat 99, E-03080 Alacant, Spain

Available online 6 May 2006

Abstract

We have developed a theoretical treatment and a simulation code to study the energy loss of swift H^+ and He^+ ion beams interacting with thin foils of different carbon allotropes. The former is based on the dielectric formalism, and the latter combines Monte Carlo with the numerical solution of the motion equation for each projectile to describe its trajectory and interactions through the target.

The capabilities of both methods are assessed by the reasonably good agreement between their predictions and the experimental results, for a wide range of projectile energies and target characteristics. Firstly, we apply the theoretical procedure to calculate the stopping cross sections for H^+ and He^+ beams in foils of different allotropic forms of carbon (such as diamond, graphite, amorphous carbon, glassy carbon and C_{60}-fullerite), as a function of the projectile energy. We take into account the electronic structure of the projectile, as well as the different charge states it can acquire, the energy loss associated to the electronic capture and loss processes, the polarization of the projectile, and a realistic description of the target.

On the other hand, the simulation code is used to evaluate the energy distributions of swift H^+ and He^+ ion beams when traversing several foils of the above mentioned allotropic forms of carbon, in order to analyze the influence of the chemical and physical state of the target in the projectile energy loss. These allotropic effects are found to become more important around the maximum of the stopping cross-section.

PACS: 34.50.Bw; 77.22.−d; 47.27.Vf; 61.46.+w

Keywords: Stopping power; Energy loss; Energy loss straggling; Dielectric properties; Allotropic effects

1. Introduction

Atomic ion beams are widely used in physics both to analyze and modify the structure of matter [1,2]. Moreover, the energy deposition by energetic ions in solid targets is a topic of great interest due to its multiple technological applications [3]. For instance, a precise knowledge of the stopping related magnitudes are important for the processing of materials by ion-beam implantation, as well as in the structural characterization of solids by ion-beam methods [4].

The energy loss of swift ions in solids significantly depends on the chemical and physical state of the target, specially when the projectile velocity is of the same order of magnitude than the mean orbital velocities of the target valence band electrons, that is, around the maximum value of the stopping power. Carbon targets are very suitable to analyze these effects because they are available in several allotropic forms, which differ from each other in their bond structure, distribution of valence electrons, density and electronic properties.

We have developed a theoretical procedure and a simulation code to study the energy loss of swift atomic ion beams incident on thin foils. In this work, we show the suitability of both treatments by comparing their results with available data from experiments.

* Corresponding author. Tel.: +34 968 367389; fax: +34 968 364148.
E-mail address: rgm@um.es (R. Garcia-Molina).

0168-583X/$ - see front matter © 2006 Elsevier B.V. All rights reserved.
doi:10.1016/j.nimb.2006.03.011

Firstly, we evaluate theoretically the electronic energy loss of swift H^+ and He^+ projectiles in the different allotropic forms of carbon (diamond, graphite, amorphous carbon, glassy carbon and C_{60}-fullerite) as a function of the projectile energy. Similar calculations were carried out and reported previously for H^+ ions in several targets [5–7], but in addition, we now take into account the different charge states the projectile can acquire when moving through the target, the energy loss associated to the electronic capture and loss processes, and the polarization of the projectile [8–10].

The second procedure to study the interaction of energetic ions with matter consists in a simulation code, which is used in this case to evaluate allotropic effects in the energy distributions of swift H^+ and He^+ ion beams incident on several allotropic forms of carbon foils. Our simulation code follows the trajectory of each projectile through the foil by solving its equation of motion, taking into account the following interactions: the stopping force due to electronic excitations (obtained from the stopping power and the energy loss straggling calculated by the previous theoretical procedure), the electronic capture and loss processes, as well as the elastic collisions with the target nuclei (treated within a Monte Carlo method [11]).

2. Projectile penetration process

When a projectile with velocity v and atomic number Z_1 enters a foil, characterized by its dielectric function ϵ, it captures or loses electrons changing its initial charge state. Once the projectile reaches the equilibrium regime, the stopping power S_p and the energy loss straggling Ω^2 of the target will be, respectively, a sum of the stopping power contributions $S_{p,q}$ and the energy loss straggling contributions Ω_q^2 due to the different charge states q that the projectile can acquire in their travel through the foil

$$S_p = \sum_{q=0}^{Z_1} \phi_q S_{p,q}, \qquad \Omega^2 = \sum_{q=0}^{Z_1} \phi_q \Omega_q^2, \tag{1}$$

where ϕ_q is the fraction of the q charge state, which depends on the target, the projectile and its velocity. Note that the summations are extended over all the possible charge states of the projectile. In what follows we use ϕ_q values obtained by using the CasP 3.1 code [12].

The dielectric formalism is used to calculate the response of the target to the passage of a fast charged projectile, which is based on a linear response of the stopping medium to the perturbation produced by the projectile charge density [13]. We have also considered the polarization of the projectile due to the electric field it induces in the target, which results in a displacement d_q between the center of the projectile electronic cloud and its nucleus. Taking into account this effect, the stopping power, $S_{p,q}$ and the energy loss straggling, Ω_q^2, for a given charge state q of the projectile, are given, respectively, by [8]

$$\begin{aligned} S_{p,q}(v) = {} & \frac{2Z_1^2e^2}{\pi v^2}\int_0^\infty \frac{dk}{k}\int_0^{kv} d\omega\,\omega\,\mathrm{Im}\left[\frac{-1}{\epsilon(k,\omega)}\right] + \frac{2e^2}{\pi v^2} \\ & \times \int_0^\infty \frac{dk}{k}\rho_q^2(k)\int_0^{kv} d\omega\,\omega\,\mathrm{Im}\left[\frac{-1}{\epsilon(k,\omega)}\right] - \frac{4Z_1e^2}{\pi v^2} \\ & \times \int_0^\infty \frac{dk}{k}\rho_q(k)\int_0^{kv} d\omega\,\omega\,\mathrm{Im}\left[\frac{-1}{\epsilon(k,\omega)}\right]\cos\left(\frac{\omega d_q}{v}\right), \end{aligned} \tag{2}$$

where e is the elementary charge, $\hbar$ is Planck's constant, $\hbar k$ and $\hbar\omega$ are, respectively, the momentum and energy transferred to the target, $\rho_q(k)$ is the Fourier transform of the projectile electronic density for the q charge state, and $\mathrm{Im}[-1/\epsilon(k,\omega)]$ is the energy loss function of the target. The expression for the energy loss straggling, Ω_q^2, is obtained from Eq. (2), replacing $d\omega$ by $d\omega(\hbar\omega)$.

The distance between the nucleus and the center of the displaced electronic cloud is given by $d_q = \alpha_q \mathscr{E}_q(v)/e$, where α_q is the projectile polarizability and $\mathscr{E}_q(v)$ is the self-induced electric field produced by the projectile

$$\mathscr{E}_q(v) = \frac{2e}{\pi v^2}\int_0^\infty \frac{dk}{k}[Z_1 - \rho_q(k)]\int_0^{kv} d\omega\,\omega\,\mathrm{Im}\left[\frac{-1}{\epsilon(k,\omega)}\right]. \tag{3}$$

Notice that for unpolarized projectiles $d_q = 0$ and then Eq. (2) reproduces the known expressions for $S_{p,q}(v)$ (analogously for the energy loss straggling) [9]. This is the case for helium, due to its small polarizability.

The charge density of the projectile is described by the statistical model proposed by Brandt and Kitagawa [14], in which the whole set of bound electrons is characterized by a generic orbital; later, Brandt [15] extended his model for projectiles with 1 or 2 bound electrons. An alternative description of the projectile charge density is made for He in several oxides [10]. Also an extension of the Brandt–Kitagawa model for Hartree–Fock densities have appeared recently in [16].

3. Dielectric response function

The electronic response of the target to an external perturbation is given by the energy loss function (ELF) of the target, which determines the probability that an inelastic event with momentum transfer $\hbar k$ and energy transfer $\hbar\omega$ takes place in the target, and contains information about the excitations that the material can sustain. The ELF is properly modelled by separating the contribution to the target electronic excitations coming from outer or inner-shell electrons, respectively [5,9,10]. The outer electron excitations are represented by a linear combination of Mermin-type ELF obtained by means of a fit of the form

$$\mathrm{Im}\left[\frac{-1}{\epsilon(k=0,\omega)}\right]_{\mathrm{outer}} = \sum_i A_i \mathrm{Im}\left[\frac{-1}{\epsilon_M(\omega_i,\gamma_i;k=0,\omega)}\right] \tag{4}$$

to the available experimental optical ELF; ϵ_M being a Mermin-type dielectric function [17] and ω_i, γ_i and A_i fitting parameters.

The excitation of the inner-shell electrons are described in terms of the generalized oscillator strengths (GOS) for isolated atoms in the hydrogenic approach. The relation between the ELF and the GOS is given by [18,19]

$$\mathrm{Im}\left[\frac{-1}{\epsilon(k,\omega)}\right]_{\mathrm{inner}} = \frac{2\pi^2\mathcal{N}}{\omega}\sum_{n\ell}\frac{\mathrm{d}f_{n\ell}(k,\omega)}{\mathrm{d}\omega}, \tag{5}$$

where $\mathcal{N}$ is the atomic density of the target and $\mathrm{d}f_{n\ell}(k,\omega)/\mathrm{d}\omega$ is the GOS of the (n,ℓ) subshell. The summation is extended over all inner subshells of the target atoms. Of course, the ionization of a given subshell can only take place if the energy transfer $\hbar\omega$ is larger than a threshold energy.

The resulting ELF must verify the f-sum rule, that is, the effective number of excited electrons per atom when $\hbar\omega \to \infty$ must tend to the total number of electrons per atom [20]. Moreover, we also calculate the mean excitation energy I of each target [20] as an additional checking of our fitted ELF, obtaining [6,7] a good agreement with the experimental data [21].

We show the optical limit of the ELF for several allotropic forms of carbon in Fig. 1. The solid lines represent our fitted ELF, with the parameters corresponding to the outer electron excitations (see Eq. (4)) given in Table 1. The symbols correspond to experimental data of the ELF [22–26]. These allotropes have distinct energy loss spectra due to their different electronic structure; for instance, the ELF of graphite, typical of a sp^2 bonding, shows two peaks, one at low energy (~7 eV) related to the π electrons plasmon, and a second peak at ~28 eV corresponding to collective excitations due to the $\pi+\sigma$ electrons; analogously, amorphous carbon, glassy carbon and C_{60}-fullerite present a similar ELF with two peaks in their energy spectra; however, diamond, with a sp^3 hybridization, only shows one peak at high energy (~35 eV).

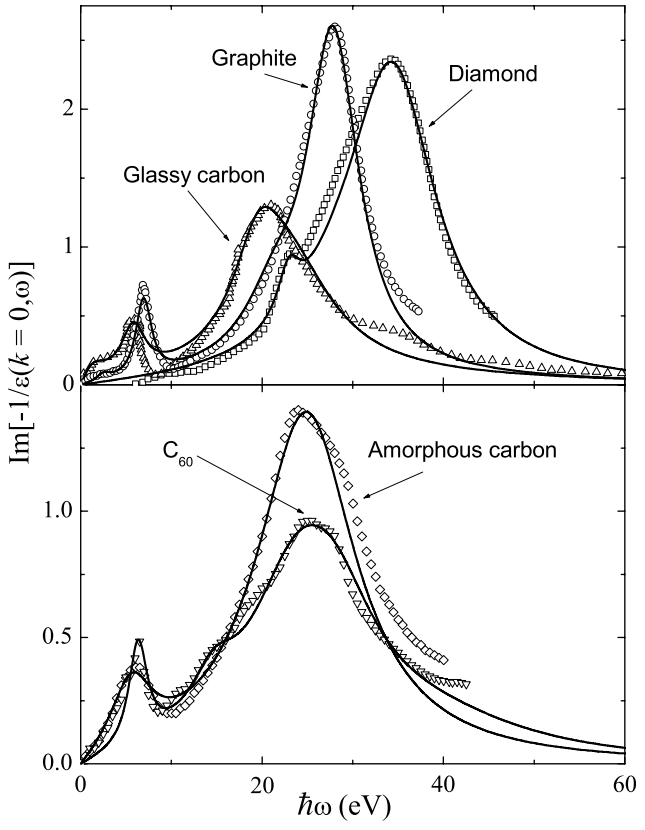

Fig. 1. Energy loss function of several carbon allotropes, in the optical limit ($k=0$), as a function of the excitation energy. Solid lines represent our model, and symbols correspond to experimental data: □ diamond [22], ○ graphite [23], ◇ amorphous carbon [24], △ glassy carbon [25], and ▽ C_{60}-fullerite [26].

Table 1
Parameters used to fit the outer electrons contribution to the optical ELF of the different allotropic forms of carbon

Target	i	$\hbar\omega_i$ (eV)	γ_i (eV)	A_i
Diamond, $D=3.515$ g/cm^3	1	22.86	2.72	4.25×10^{-2}
	2	29.93	13.61	1.57×10^{-1}
	3	34.77	11.43	6.98×10^{-1}
Graphite, $D=2.25$ g/cm^3	1	2.58	1.36	2.77×10^{-2}
	2	6.99	1.77	1.51×10^{-1}
	3	21.77	8.16	1.56×10^{-1}
	4	28.03	6.80	5.94×10^{-1}
	5	38.09	68.03	7.12×10^{-2}
Amorphous carbon, $D=1.7$ g/cm^3	1	6.26	5.71	2.36×10^{-1}
	2	25.71	13.33	7.09×10^{-1}
Glassy carbon, $D=1.459$ g/cm^3	1	2.31	4.22	1.80×10^{-1}
	2	5.99	2.99	1.76×10^{-1}
	3	19.86	6.45	$1.97\times;10^{-1}$
	4	23.67	12.38	3.96×10^{-1}
	5	38.09	54.42	7.65×10^{-2}
C_{60}-fullerite, $D=1.678$ g/cm^3	1	6.45	2.45	1.53×10^{-1}
	2	14.97	6.26	7.37×10^{-2}
	3	24.49	13.06	2.92×10^{-1}
	4	28.57	12.24	1.73×10^{-1}
	5	40.82	27.21	8.49×10^{-2}

D is the mass density of the target.

4. Simulation code

Our simulation code, described in more detail elsewhere [27,28], dynamically follows the evolution of each projectile, providing at any time its position, velocity and charge state. These data are used to evaluate the energy loss distributions of the projectiles that leave the foil and reach a detector with specific characteristics (such as position, angular acceptance, etc.). We take into account the continuous slowing down of the projectile due to electronic interactions together with elastic collisions with the target nuclei [11]. As the energy loss depends on the charge state of the projectile, we have also included the possibility of electron capture or loss by the atomic projectiles. By doing this we take into account the energy loss due to electron capture and loss processes, as well as the transient time required to reach the charge state equilibrium [29], which can be important in very thin foils.

The elastic collisions with atomic nuclei are incorporated in the simulation via a Monte Carlo code, where the nuclear energy loss is also considered. This code describes consecutive binary collisions, using the universal potential [30] as the ion-atom potential. The mean free path between successive collisions, and the corresponding collision angles, are chosen statistically by means of a Monte Carlo method [31].

At each time step the electronic stopping force is statistically obtained from a Gaussian distribution, whose mean value (stopping power) and variance (energy loss straggling) are calculated from the dielectric formalism and the ELF description previously described. The stopping power and the energy-loss straggling depend on the instantaneous projectile velocity.

5. Results and discussions

In order to study the slowing down of H^+ and He^+ ions through a solid we use the stopping cross section (SCS), which is a more convenient magnitude than the stopping power, because the SCS only depends on the strength of the interactions, and not on the atomic density of the target [32]. Note that getting rid of the dependence on the atomic target density is specially convenient to analyze allotropic effects. The SCS is defined as $\mathrm{SCS} = S_p M_2/D$, where D and M_2 are, respectively, the mass density and the atomic mass of the target.

In Fig. 2 we depict the SCS for H^+ and He^+ ion beams impinging in different carbon foils, as a function of the incident projectile energy. We use Eqs. (1) and (2) with the previous representations of the ELF and the projectile charge density $\rho_q(k)$ from the modified Brandt and Kitagawa model [14,15]. We have assumed the same values of the charge state fractions for all these allotropes, which are obtained from the code CasP 3.1 [12], because they change very little for the different forms of carbon. These calculations include the effects due to polarization of the projectile [9], and the SCS contribution associated to electronic capture and loss processes, which is estimated extending the model proposed in [8].

Our theoretical results (lines in the figures) compare fairly well with experimental data, denoted by symbols [33]. At low and intermediate projectile energies, where the SCS strongly depends on the target chemical state, we obtain that SCS (diamond) < SCS (C_{60}-fullerite) < SCS

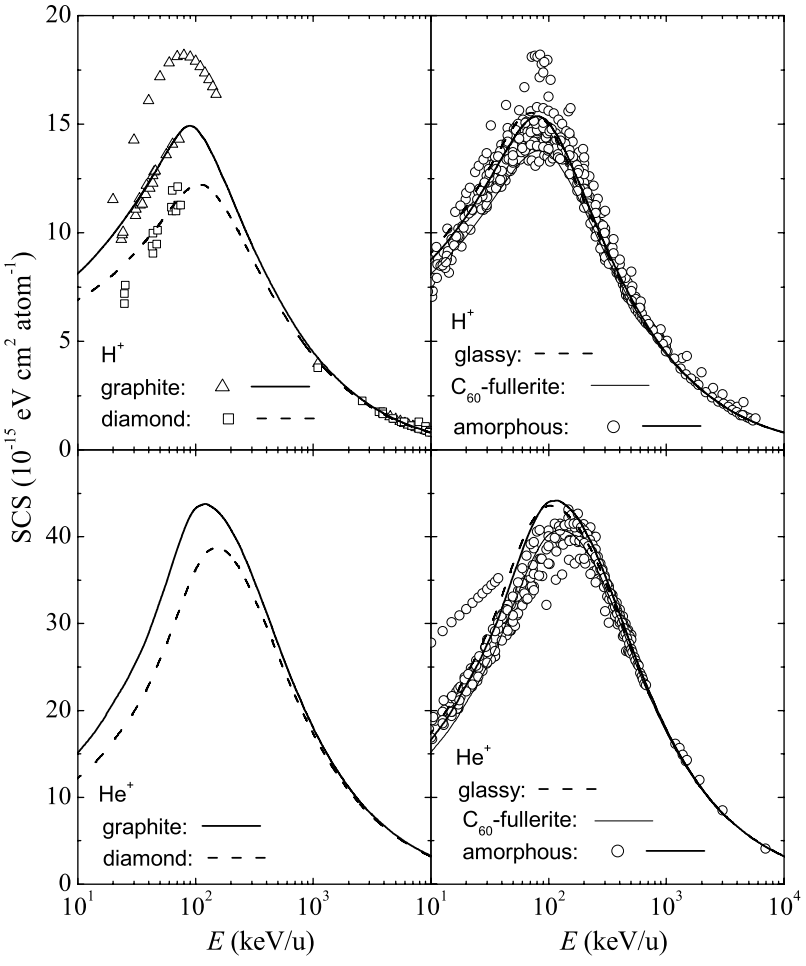

Fig. 2. Electronic stopping cross-section (SCS) for H^+ and He^+ in several allotropic carbon foils as a function of the projectile energy. Lines represent our results and symbols correspond to experimental data compiled in [33].

(graphite) < SCS (amorphous carbon) < SCS (glassy carbon), while at high energies the SCS values are similar for all the carbon foils.

The allotropic effects in the electronic energy loss of H^+ and He^+ are due to the differences in the energy loss function of each allotropic form of carbon. The ELF of the inner-shell electrons are the same for all allotropic carbon foils, but there are important differences on the ELF of the valence band electrons (see Fig. 1). According to the strength of the interaction for each allotropic form, only some of the valence band electrons can be excited by a projectile with low or intermediate energies, whereas all the valence band electrons can be excited by a projectile with high energy, independently of the target allotropic form; so this explain the same SCS obtained at high projectile energies for all allotropic forms of the target.

Although diamond and graphite present an energy gap in its electronic spectrum (4 eV and 1 eV, respectively) it is not relevant in the energy loss of H^+ and He^+ projectiles for this energy range. Furthermore, we have found that for initial energies higher than 300 keV/u the influence of the K-inner-shell electron excitation in the SCS becomes important; for example, their contribution is ~12% of the total SCS for energies ~1 MeV/u. The semiempirical SRIM code [34], although widely used in the literature for comparison, is not able to distinguish between the SCS of the different allotropic forms of carbon, so it was not included in this analysis.

In order to analyze the allotropic effects on the energy distributions of H^+ and He^+ ions beams we have used the computer code, previously described, to calculate the energy distribution in the forward direction of H^+ and He^+, respectively, after traversing thin films of diamond, graphite, amorphous carbon, glassy carbon and C_{60}-fullerite. These distributions are depicted in Fig. 3 for a projectile incident energy of 100 keV/u, around the maximum of the stopping cross-section, and for a foil thickness of 200 Å. All energy distributions are normalized to unit area. Note that the projectile energy distribution in diamond is systematically shifted to lower energies with respect to graphite and amorphous carbon. Also, the energy distributions are wider for diamond than that for graphite and amorphous carbon. The energy distributions we obtain for glassy carbon and C_{60}-fullerite are very similar, because their similar ELFs (see Fig. 1), so we do not present the results obtained for glassy carbon for clarity reasons.

The observed allotropic effects in the energy distribution are mainly due to the different values of the SCS for each allotropic carbon foil, because we have checked that the energy loss straggling, normalized to the target density is similar for all allotropic forms of carbon, even at low projectile energies. These allotropic effects depend on both the ELF of the carbon foils and the target density. We have calculated the energy distributions for other foil thicknesses and incident projectile energies and they show the same trend as in Fig. 3.

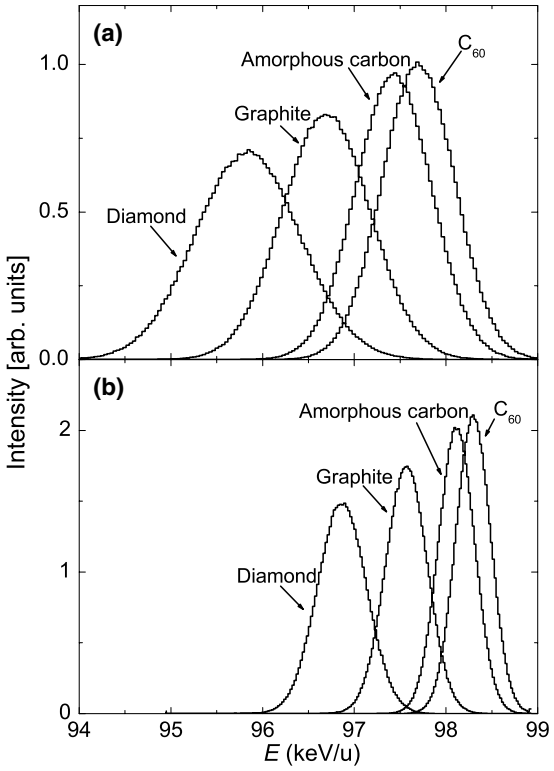

Fig. 3. Energy distributions in the forward direction of (a) H^+ and (b) He^+ ion beams transmitted through foils of different allotropic forms of carbon. The incident energy is 100 keV/u and the foil thickness is 200 Å.

The differences between the average energies of the energy distributions for the different carbon foils decrease when the initial energy of the projectile increases, because the similar SCS values for high projectile energies. As expected, the average energy of the energy distributions decreases and becomes wider the thicker is the foil, because the larger path of the projectile through the target. In order to check the capability of our simulation code, it was applied to reproduce the experimental energy distributions of 56.3 keV H^+ ion beam through an 128 Å amorphous carbon foil [35], showing a quite good agreement [11]. Note that nowadays it is not possible to make self-supported thin foils for some of the allotropic forms of carbon presented in this work, so actually transmission energy loss distributions of these materials cannot be obtained experimentally; nevertheless we have made these calculations in order to show the capabilities of our simulation code.

Finally, we show in Fig. 4 the SCS-ratio defined as the SCS of each allotropic carbon foil divided by the SCS of graphite, as a function of the initial energy for H^+ and He^+ ion beams, respectively. The lines are the calculated SCS-ratios, which are evaluated from the average energy of the projectile energy distributions. The symbols are the experimental data for diamond [32,36,37] and amorphous carbon [38]. It can be seen that our calculations agree fairly well with the available experimental data (taking into account their error bars).

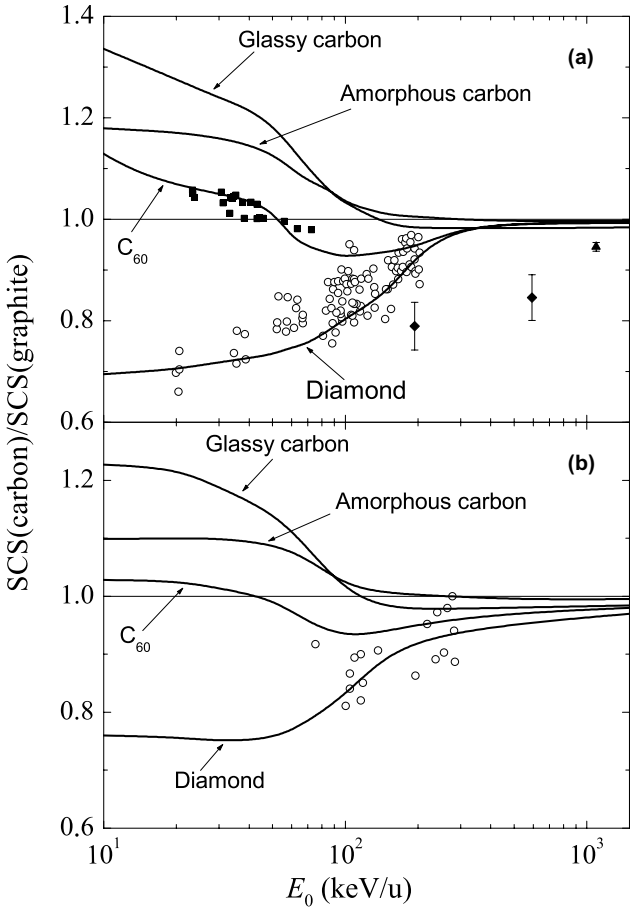

Fig. 4. Stopping cross-section ratio for several carbon allotropes, as a function of the projectile energy for (a) H^+ and (b) He^+. Solid lines represent our results and symbols are experimental data: diamond (○ [32], ▲ [36], ♦ [37]) and amorphous (■ [38]).

We found that the SCS of amorphous carbon (glassy carbon) for H^+ ions is up to 15% (22%) larger than that of graphite at intermediate energies (~10 keV/u). Moreover, the SCS of diamond is 27% lower than the SCS of graphite. In the case of C_{60}-fullerite there are not significant differences. These allotropic effects decrease when increasing the initial projectile energy, as the SCS-ratio tending to unity shows. The same number of electrons contribute to the excitation for all the allotropic forms of carbon at higher energies. The fact that the SCS of diamond is lower than that of graphite in the whole energy range can be understood by observing their ELF in Fig. 1, the ELF of graphite being displaced toward lower values of the excitation energy $\hbar\omega$. The same conclusions can be drawn for the case of He^+ projectiles. It is worth to notice that similar allotropic effects were also observed for carbon projectiles [39].

The main discrepancies between our results and the experimental data appear for the SCS-ratio of amorphous carbon in the case of H^+ projectiles. This disagreement could be attributed to the differences between the characteristics of the amorphous carbon foils used in [38] to obtain the SCS and the one used in [24] to obtain the ELF, which was used in our calculations. Fig. 2 shows that there is a high dispersion in the experimental data for the SCS of amorphous carbon, which implies a high dispersion of the SCS ratio in Fig. 4, this makes our calculations of the SCS ratio inside the experimental dispersion. Further experimental results would be desirable to elucidate this question.

6. Conclusions

We have presented a theoretical treatment and a simulation code to evaluate the energy loss of swift H^+ and He^+ ion beams through thin foils.

Firstly, we have applied the theoretical procedure to calculate the SCS of different allotropes of carbon (such as diamond, graphite, amorphous carbon, glassy carbon and C_{60}-fullerite) for H^+ and He^+ beams as a function of the projectile energy. We have taken into account the projectile electronic structure, the different charge states the projectile can acquire, the energy loss associated to the electronic capture and loss processes, the polarization of the projectile, and a realistic description of the target. Theoretical results for both type of targets agree fairly well with the experimental data.

On the other hand, the simulation code is used to evaluate the energy distributions of swift H^+ and He^+ ion beams when traversing several allotropic carbon foils. Significant allotropic effects in the SCSs at intermediate projectile energies are obtained, but they disappear as the projectile energy increases, where all SCSs tend to the same value whatever the allotropic form of the target is. Our results are in good agreement with the available experimental data, and provide a clear evidence of how the chemical and physical state of the carbon foils affect the slowing down of swift projectiles.

Acknowledgements

This work was supported by the Spanish Ministerio de Educación y Ciencia (projects BFM2003-04457-C02-01 and BFM2003-04457-C02-02). S.H.A. thanks Fundación Cajamurcia for a postdoctoral grant. C.D.D. thanks the Spanish Ministerio de Educación y Ciencia for support under the Ramón y Cajal Program.

References

[1] M.A. Kumakhov, F.F. Komarov, Energy Loss and Ion Ranges in Solids, Gordon and Breach, New York, 1981.
[2] R. Kelly, M.F. da Silva (Eds.), Material Modification by High-Fluence Ion Beams, NATO ASI Series E: Applied Sciences, Vol. 155, Kluwer, Dordrecht, 1989.
[3] S.A. Campbell, The Science and Engineering of Microelectronic Fabrication, Oxford University, Oxford, 1996.
[4] A. Gras-Martí, H.M. Urbassek, N.R. Arista, F. Flores (Eds.), Interaction of Charged Particles with Solids and Surfaces, NATO ASI Series B: Physics, Vol. 271, Plenum, New York, 1991.
[5] I. Abril, R. Garcia-Molina, C.D. Denton, F.J. Pérez-Pérez, N.R. Arista, Phys. Rev. A 58 (1998) 357.
[6] J.C. Moreno-Marín, I. Abril, R. Garcia-Molina, Nucl. Instr. and Meth. B 193 (2002) 30.

[7] R. Garcia-Molina, I. Abril, C.F. Sanz, N.R. Arista, Nucl. Instr. and Meth. B 190 (2002) 89.
[8] S. Heredia-Avalos, R. Garcia-Molina, Nucl. Instr. and Meth. B 193 (2002) 15.
[9] S. Heredia-Avalos, J.C. Moreno-Marín, I. Abril, R. Garcia-Molina, Nucl. Instr. and Meth. B 230 (2005) 118.
[10] S. Heredia-Avalos, R. Garcia-Molina, J.M. Fernández-Varea, I. Abril, Phys. Rev. A 72 (2005) 052902.
[11] C.D. Denton, R. Garcia-Molina, I. Abril, N.R. Arista, Nucl. Instr. and Meth. B 135 (1998) 45.
[12] P.L. Grande. G. Schiwietz, CasP, Convolution approximation for swift Particles, version 3.1, 2004. Code available from: <http://www.hmi.de/people/schiwietz/casp.html>.
[13] J. Lindhard, K. Dan, Vidensk. Selsk. Mat.-Fys. Medd. 28 (8) (1954).
[14] W. Brandt, M. Kitagawa, Phys. Rev. B 25 (1982) 5631.
[15] W. Brandt, Nucl. Instr. and Meth. 194 (1982) 13.
[16] J.A.M. Pereira, Abstract 102, Proceedings of the XVII International Conference on Ion Beam Analysis, Seville, Spain, 2005.
[17] N.D. Mermin, Phys. Rev. B 1 (1970) 2362.
[18] U. Fano, Ann. Rev. Nucl. Sci. 13 (1963) 1.
[19] R.F. Egerton, Electron Energy-Loss Spectroscopy in the Electron Microscope, Plenum Press, New York, 1989.
[20] E. Shiles, T. Sasaki, M. Inokuti, D.Y. Smith, Phys. Rev. B 22 (1980) 1612.
[21] ICRU Report 49, Stopping Powers and Ranges for Protons and Alpha Particles, International Commission on Radiation Units and Measurements, Bethesda, 1993.
[22] J. Daniels, C.V. Festenberg, H. Raether, K. Zeppenfeld, in: G. Hohler (Ed.), Springer Track in Modern Physics, Vol. 54, Springer-Verlag, Berlin, 1970, p. 78.
[23] R. Raether, Excitations of Plasmons and Interband Transitions by Electrons, Springer Tracts in Modern Physics, Vol. 88, Springer, Berlin, 1980.
[24] J. Cazaux, D. Gramari, J. Phys. 38 (1977) L133.
[25] M.W. Williams, E.T. Arakawa, J. Appl. Phys. 43 (1972) 3460.
[26] R. Kuzuo, M. Terauchi, M. Tanaba, Y. Saito, H. Shinohara, Jap. J. Appl. Phys. 30 (1991) L1817.
[27] C.D. Denton, R. Garcia-Molina, I. Abril, N.R. Arista, Nucl. Instr. and Meth. B 135 (1998) 50.
[28] R. Garcia-Molina, C.D. Denton, I. Abril, N.R. Arista, Phys. Rev. A 62 (2000) 012901.
[29] R. Garcia-Molina, S. Heredia-Avalos, Phys. Rev. A 63 (2001) 044901.
[30] J.F. Ziegler, J.P. Biersack, U. Littmark, The Stopping and Ranges of Ions in Matter, Plenum, New York, 1985.
[31] W. Moller, G. Pospiech, G. Schrieder, Nucl. Instr. and Meth. B 130 (1975) 265.
[32] W. Käferböck, W. Rössler, V. Necas, P. Bauer, M. Penãlba, E. Zarate, A. Arnau, Phys. Rev. B 55 (1997) 13275.
[33] H. Paul, Experimental stopping power compilation. Available from: <http://www.exphys.uni-linz.ac.at/Stopping/>.
[34] SRIM, The Stopping and Range of Ions in Matter. Available from: <http://www.srim.org>.
[35] J.H. Ormrod, H.E. Duckworth, Can. J. Phys. 41 (1963) 1424.
[36] S.D. Softky, Phys. Rev. 123 (1961) 1685.
[37] V.S. Kulikauskas, F.G. Neshov, A.A. Puzanov, A.R. Urmanov, V.P. Shubin, Pisma V. Zh. Tekhnicheskoi Fiziki 10 (1984) 111.
[38] V. Necas, W. Käferböck, W. Rössler, P. Bauer, Nucl. Instr. and Meth. B 80–81 (1993) 41.
[39] W.Y. Baek, G.H. Both, D. Gassen, W. Neuwirth, M. Zielinski, Phys. Rev. A 35 (1987) 51.